Intrinsic and impurity luminescence of CaF$_2$, CaF$_2$:Eu^{2+} and CaF$_2$:Eu^{3+} nanoparticles at high energy excitation

A.V.Zhyshkovych, V.V.Vistovskyy, N.E.Mitina[*], A.S.Zaichenko[*], A.V.Gektin[**], A.S.Voloshinovskii

I.Franko National University of Lviv, 8a Kyryla i Mefodiya St., 79005 Lviv, Ukraine
[*]Lviv Polytechnic National University, 12 S.Bandera St., 79013 Lviv, Ukraine
[**]Institute for Scintillation Materials, STC "Institute for Single Crystals", National Academy of Sciences of Ukraine, 60 Lenin Ave., 61001 Kharkiv, Ukraine

CaF$_2$, CaF$_2$:Eu^{2+} and CaF$_2$:Eu^{3+} nanoparticles were synthesized by the chemical sedimentation method. The study of intrinsic and impurity recombination luminescence of the nanoparticles was carried out using synchrotron radiation. The intrinsic and impurity luminescence intensity was found to depend significantly on the nanoparticles size. The surface defects, the ratio between the thermalization length of photoelectrons and the nanoparticle size are crucial for luminescence intensity of the nanoparticles. The luminescence caused by the charge-transfer to Eu^{3+} ions is dominant for the small size nanoparticles.

Наночастицы CaF$_2$, CaF$_2$:Eu^{2+} и CaF$_2$:Eu^{3+} синтезированы методом химического осаждения. Исследование собственной и примесной рекомбинационной люминесценции наночастиц проведено с использованием синхротронного излучения. Выявлена значительная зависимость интенсивности собственной и примесной люминесценции от размеров наночастиц. Поверхностные дефекты, длина термализации фотоэлектрона и размер наночастицы являются определяющими для интенсивности люминесценции наночастиц. Люминесценция с переносом заряда к Eu^{3+} ионам преобладает для наночастиц малых размеров.

Власна та домішкова люмінесценція наночастинок CaF$_2$, CaF$_2$:Eu^{2+} та CaF$_2$:Eu^{3+} при високоенергетичному збудженні. А.В.Жишкович, В.В.Вістовський, Н.Є.Мітіна, О.С.Заіченко, О.В.Гектін, А.С.Волошиновський.
Наночастинки CaF$_2$, CaF$_2$:Eu^{2+} та CaF$_2$:Eu^{3+} синтезовано методом хімічного осадження. Дослідження власної та домішкової рекомбінаційної люмінесценції наночастинок проведено з використанням синхротронного випромінювання. Виявлено значну залежність інтенсивності власної та домішкової люмінесценції від розмірів наночастинок. Поверхневі дефекти, співвідношення між довжиною термалізації фотоелектрона та розміром наночастинки є визначальними для інтенсивності люмінесценції наночастинок. Люмінесценція з перенесенням заряду до Eu^{3+} іонам є переважаючою для наночастинок малих розмірів.

1. Introduction

Crystals of pure and impurity doped fluorides (such as BaF_2, CaF_2, SrF_2) are traditional objects of research for study of the mechanism of scintillation processes. At the same time, some of them exhibit the acceptable scintillation parameters. Thus, for example, a scintillator based on CaF_2:Eu^{2+} demonstrates a light yield about 19,000 photons/MeV [1] and BaF_2 crystals — 10,000 photons/MeV for self-trapped exciton (STE) luminescence with decay time of 600 ns and 1,800 photons/MeV for core-valence luminescence ($\lambda = 225$ nm, $\tau = 0.9$ ns) [2]. Also, there are publications, in which it is reported a relatively high light yield for SrF_2 — 18,000 photons/MeV and SrF_2:Ce — 8,600 photons/MeV [3].

In recent years, the possibility of nanocrystal applying for new composite scintillation materials creation is quite actively discussed [4]. Such nanosize scintillators could partially replace to some extent the traditional crystal scintillation materials, production technology of which is quite expensive. The luminescent nanoparticles can find its application as: the additives to polymeric films for X-ray registration, the luminescent markers for biomedical researches and the nanoscintillators for photodynamic radiotherapy [5]. For these aims it is necessary to use the nanoparticles of small size demonstrating the desirable light yield. Therefore, the researches aimed to elucidate the regularities of high-energy radiation interaction with the nanoparticles are actual. One of these research aspects is the clarification of luminescence intensity dependence on the nanoparticles size and on the energy of excitation quanta, and in particular the analysis of intrinsic and impurity recombination luminescence intensity. From this point of view, the CaF_2 nanoparticles doped with Eu^{3+} and Eu^{2+} ions may attract attention as nanoscintillators for photodynamic therapy and the luminescent biomarkers which can be exited by the optical and X-ray quanta. High penetration ability of X-rays and overlapping of CaF_2:Eu^{3+} and CaF_2:Eu^{2+} nanoparticle emission with the transparency range of the biological tissue may allow the visualization of the processes deeply inside of tissue.

2. Experimental

CaF_2:Ln (Ln = Eu^{3+}, Eu^{2+}) nanoparticles were synthesized from aqueous solutions of $CaCl_2$, $LnCl_3$ and NH_4F salts in the presence
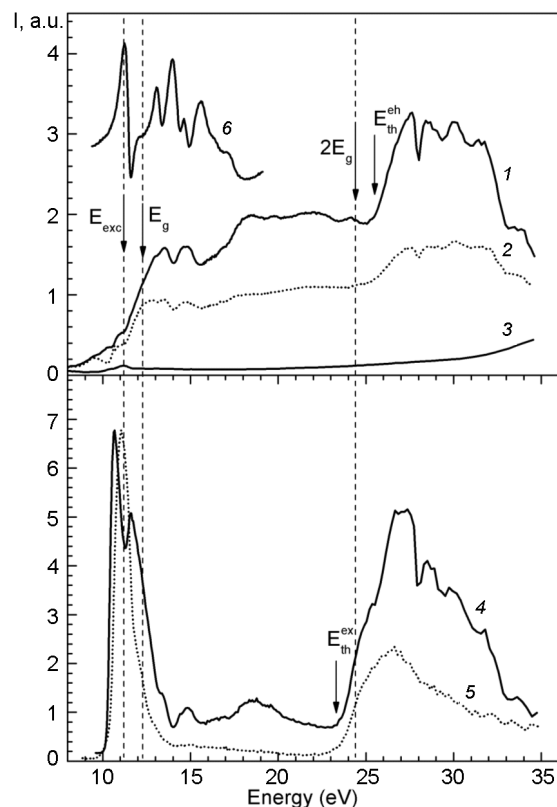

Fig. 1. Luminescence excitation spectra of europium ions in CaF_2:Eu^{2+} nanoparticles with the average size 140 nm (curve *1*), 50 nm (curve *2*) and 20 nm (curve *3*) for $\lambda_{em} = 425$ nm. The normalized STE luminescence excitation spectrum of CaF_2 nanoparticles — 140 nm (curve *4*) and 20 nm (curve *5*) for $\lambda_{em} = 300$ nm. The reflection spectrum of the bulk CaF_2 crystal (curve *6*).

of ethanol to slow down the chemical reaction speed with the purpose to reduce nanoparticle size [6, 8]. Water solution of $CaCl_2$ was slowly added with 1 drop/s rate to the solution of NH_4F at vigorous mixing. As a result a white fine-dispersed precipitation was obtained. The precipitation was separated by centrifuge and washed out by distilled water several times to the neutral pH value. The CaF_2:Ln nanoparticles obtained were dried under vacuum to constant weight. In order to obtain the nanoparticles of different size the samples were annealed at different temperatures. The nanoparticles sizes were determined by X-ray diffraction method, evaluating the diffraction peak width and using Scherrer equation. The typical average sizes of the nanoparticles are 20÷140 nm.

Luminescence studies of CaF_2, CaF_2:Eu^{3+} and CaF_2:Eu^{2+} nanocrystals were performed

using synchrotron radiation at SUPERLUMI station of HASYLAB (DESY, Hamburg) [7]. The luminescence excitation spectra were measured upon excitation with the quanta energy range 4÷40 eV and the spectral resolution of 0.3 nm. The luminescence spectra were registered in the range of 200÷800 nm with the resolution of ~2 nm. All measurements were performed at room temperature.

3. Results and discussion

3.1. Luminescence properties of CaF$_2$ and CaF$_2$:Eu^{2+} nanoparticles

In the STE luminescence excitation spectrum (λ_{em} = 300 nm) of the CaF$_2$ nanoparticles one can distinguish several spectral energy ranges (Fig. 1, curves 4 and 5). The first energy range of the spectrum, which is responsible for the optical mechanism of STE creation ($h\nu < E_g$ = 12.1 eV), is the most effective for the STE excitation. Also, the high intensity of the STE excitation occurs in the range of multiplication of the electronic excitations ($h\nu > E_g + E_{ex}$). The threshold of the electronic excitations growth, which is observed in this range, is in a good agreement with the energy $h\nu = E_g + E_{ex}$ = 23.3 eV and is a result of photoelectron scattering on the valence electrons with the creation of secondary excitations [9]. Detailed mechanism of the STE luminescence excitation of the CaF$_2$ nanoparticles is discussed in [8].

The luminescence excitation intensity reflects the tendency of intensity decrease with the nanoparticles size reduction (Fig. 1, curves 4 and 5). In the range of electron-hole pair creation ($E_g < h\nu < 2E_g$) the luminescence excitation is less effective. Here, the intrinsic luminescence intensity decreasing is caused by the photoelectron thermalization length exceeding of the nanoparticles size [8].

Upon excitation in the range of band-to band transitions of CaF$_2$ matrix ($h\nu$ > 12.1 eV), one can observe the band at 425 nm in the CaF$_2$:Eu^{2+} nanoparticle luminescence spectra (Fig. 2), which is attributed to $4f^65d^1 \rightarrow 4f^7$ transition in Eu^{2+} ions. The STE luminescence intensity of CaF$_2$ and 425 nm band of the CaF$_2$:Eu^{2+} nanoparticles reveal a similar dependence on the nanoparticle size reduction. Thus, the luminescence intensity of CaF$_2$:Eu^{2+} nanoparticles significantly decreases with the nanoparticle size reduction (Fig. 2) and the luminescence is almost absent for the
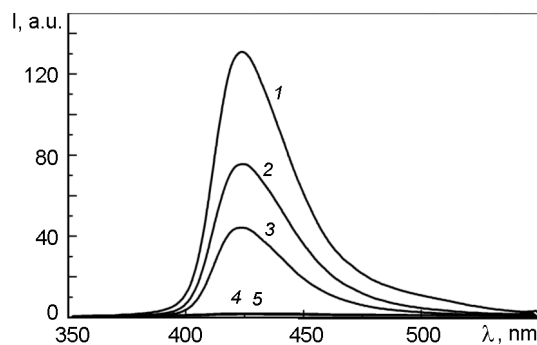

Fig. 2. Luminescence spectra of CaF$_2$:Eu^{2+} for different nanoparticles sizes ($h\nu_{exc}$ = 20.6 eV). The average nanoparticles size: 1 – 140 nm, 2 – 80 nm, 3 – 50 nm, 4 – 28 nm, 5 – 20 nm.
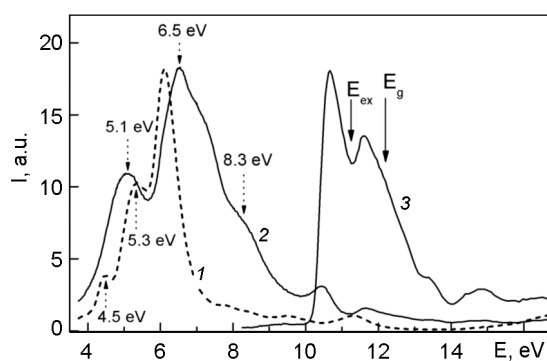

Fig. 3. Normalized luminescence excitation spectra of Eu^{3+} center emission at 620 nm in CaF$_2$:Eu^{3+} and STE (300 nm) in CaF$_2$ (curve 3). The average nanoparticles size: 20 nm (curve 1), 140 nm (curves 2 and 3).

small nanoparticles with size $a < 50$ nm in the band-to-band excitation range (Fig. 2, curves 4 and 5). Such a behaviour can be explained by the increasing of surface defects quantity with the nanoparticles size reduction and the photoelectron thermalization length exceeding of the nanoparticles size.

The luminescence excitation spectra of Eu^{2+} centers (Fig. 1, curves 1, 2 and 3) also demonstrate the tendency of luminescence intensity decreasing with the nanoparticle size reduction. The luminescence excitation spectra of the CaF$_2$:Eu^{2+} nanoparticles reveal a regularity which is characteristic for the recombination luminescence mechanism in the case of electron-hole pair recombination with the Eu^{2+} centers. At such excitation luminescence mechanism the main growths of luminescence occurs in the case of electrons and holes formation in the conduction and valence band providing $h\nu > E_g$. The luminescence excitation threshold
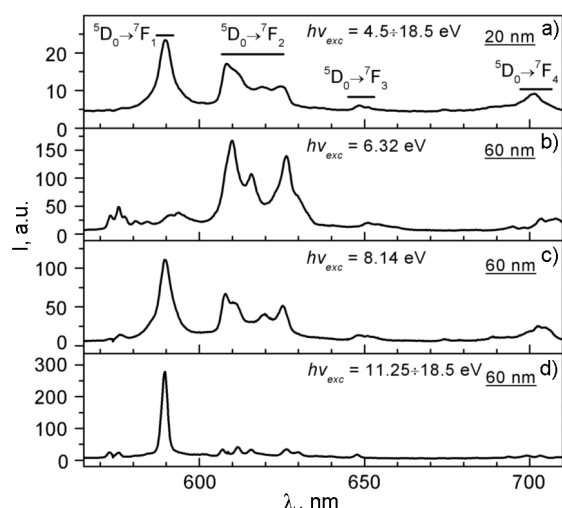
Fig. 4. Luminescence spectra of $CaF_2:Eu^{3+}$ for 20 nm (a) and 60 nm (b, c, d) nanoparticles sizes at different excitation energies.

related to electronic excitation multiplication in the case of formation of secondary electron-hole pairs is observed at energies $h\nu \geq 25.4$ eV, which slightly exceeds $2E_g$. The position of this threshold coincides with the threshold of electronic excitations multiplication in $CaF_2:Eu^{2+}$ bulk crystals [9].

3.2. Luminescence properties of $CaF_2:Eu^{3+}$ nanoparticles

The luminescence spectra show the typical Eu^{3+} ion lines in the red spectral area. These lines correspond to transitions from the excited $^5D_0$ level to ^7F_j ($J = 0,...,6$) levels of $4f^6$ configuration [11]. In the case of $CaF_2:Eu^{3+}$ nanoparticles the luminescence spectra demonstrate dependence on the nanoparticle size and the exciting energy of quantum (Fig. 4). In order to elucidate the optimal condition for the Eu^{3+} ion luminescence, the luminescence excitation spectra of CaF_2 at 300 nm (Fig. 3, curve 3) and $CaF_2:Eu^{2+}$ at 620 nm (Fig. 3, curve 1) for large nanoparticles ($a = 140$ nm) were compared. As it can be seen in Fig. 3, the Eu^{3+} luminescence in the CaF_2 nanoparticres with size of $a = 140$ nm is efficiently excited in transparency range of the nanoparticles at $h\nu < 10$ eV. Moreover, the Eu^{3+} luminescence intensity is low in the case of photon quanta energy 10 eV $< h\nu < E_g = 12.1$ eV. Thus, the excitation via energy transfer from STE to Eu^{3+} ions is insignificant. For band-to-band transition range ($h\nu > E_g$) the Eu^{3+} ion luminescence is also ineffective, this feature

of luminescence intensity is observed in the bulk crystals too [10].

Available information concerning the europium ion excitation in the transparency range of the matrix allows to attribute the transitions in the near exciton range of the $CaF_2:Eu^{3+}$ nanoparticles (Fig. 3). According to [12] the absorption spectrum of the $CaF_2:Eu^{3+}$ bulk crystal reveals two charge-transfer bands (CT) from fluorine to europium ions at 6.85 eV (CT_2) and 8.35 eV (CT_1). We can also observe two bands at ~8.3 eV and ~6.5 eV in the luminescence excitation spectrum of the $CaF_2:Eu^{3+}$ nanoparticles which can be attributed to the charge-transfer bands. From this point of view a band at ~8.3 eV is caused by the charge transfer involving the fluorine ions in regular lattice and the second one at ~6.5 eV is by the charge-transfer from interstitial fluorine ion to europium ion. In addition there is a band at ~5.1 eV ($a = 140$ nm), which is not present in the bulk crystals, perhaps it is a result of the charge-transfer involving the oxygen ions [13].

For small $CaF_2:Eu^{3+}$ nanoparticles ($a = 20$ nm) the charge-transfer band involving the regular fluorine ions is practically absent, and the charge-transfer bands involving interstitial fluorine and oxygen ions are predominant in the spectrum (Fig. 3, curve 1). The observed bands could be conditionally ascribed to the charge transfer involving the fluorine surface defects (band at ~6.1 eV) and oxygen defects (band at ~5.3 eV and ~4.5 eV).

The structure of $4f-4f$ luminescence spectrum of Eu^{3+} ion strongly depends on local symmetry of the Eu^{3+} center. This circumstance allows the revealing of the Eu^{3+} centers with different symmetry in the crystal lattice [12]. In the $CaF_2:Eu^{3+}$ nanoparticles with size of $a > 40$ nm (Fig. 4, b, c, d) one can observe two different the Eu^{3+} centers with O_h and C_{4v}-symmetry. The formation of such symmetry centers is typical in the case of lanthanide ions doped into fluoride crystals [12]. In the case of O_h-symmetry centers one can observe the dominant band caused by $^5D_0 \rightarrow {}^7F_1$ transition, and for C_{4v}-symmetry $^5D_0 \rightarrow {}^7F_2$ transition band is predominant. Such relation between the manifestation of $^5D_0 \rightarrow {}^7F_1$ and $^5D_0 \rightarrow {}^7F_2$ transitions is in a good agreement with selection rules for magnetic-dipole and electric-dipole transitions. For the cubic centers with the inversion symmetry the magnetic-dipole $^5D_0 \rightarrow {}^7F_1$ transitions are dominated by the luminescence intensity. In addition, when

the symmetry is reduced and the inverse center is absent, the electric-dipole $^5D_0 \rightarrow {}^7F_2$ transition predominates [11].

The O_h–Eu^{3+} centers with dominating band at 590 nm ($^5D_0 \rightarrow {}^7F_1$) are mainly excited in the transparency range of the CaF_2 nanoparticles ($a > 40$ nm) in the charge-transfer band involving F^- ions located in regular positions (8.1 eV). Meanwhile, the C_{4v}–Eu^{3+} centers revealing the dominating band at 620 nm ($^5D_0 \rightarrow {}^7F_2$) are mainly excited in the band peaked at 6.8 eV and is caused by the charge-transfer from F^- ions located in the interstitial lattice sites.

The band peaked at 590 nm dominates in the emission spectra under excitation in the fundamental absorption range of the CaF_2 matrix. As the size of nanoparticles is reduced $a < 40$ nm (Fig. 4a) the luminescence spectra shape does not reveal the dependence on excitation energy and demonstrate the commensurability of intensity of $^5D_0 \rightarrow {}^7F_1$ and $^5D_0 \rightarrow {}^7F_2$ transition attributed to the centers with O_h and C_{4v}-symmetry, respectively. Such luminescence spectrum behaviour indicates that the luminescence from the low symmetry centers excited with the charge-transfer from oxygen ion to europium ion is predominant for the small nanoparticles ($a < 40$ nm).

4. Conclusions

CaF_2, CaF_2:Eu^{2+} and CaF_2:Eu^{3+} nanoparticles with size of 20÷140 nm were synthesized by the chemical sedimentation method. The STE luminescence intensity of the CaF_2 nanoparticles significantly decreases with reduction of the nanoparticle size. Such dependence is caused by the photoelectron thermalization length exceeding the nanoparticles size. In this case the electron can leave the nanoparticle or be captured by the surface defects. These reasons lead to the decreasing of recombination luminescence intensity of impurity centers in the CaF_2:Eu^{2+} and CaF_2:Eu^{3+} nanoparticles. The Eu^{3+} ions in CaF_2:Eu^{3+} nanoparticles create the O_h and C_{4v}-symmetry centers. The luminescence of Eu^{3+} centers excited in the range of charge-transfer transitions is less sensitive to the nanoparticle size reduction. The luminescence of the Eu^{3+} centers with charge-transfer from the impurity oxygen ions to Eu^{3+} ions is predominant in the small CaF_2:Eu^{3+} nanoparticle, and itself centers have C_{4v}-symmetry.

References

1. http://www.detectors.saint-gobain.com/CaF2.aspx
2. http://www.detectors.saint-gobain.com/BaF2.aspx
3. R.Shendrik, E.A.Radzhabov, A.I.Nepomnyashchikh, *Radiat. Meas.*, **56**, 58 (2013).
4. E.A.McKigney, R.E.Del Sesto, L.G.Jacobsohn et al., *Nucl. Instrum. Meth. Phys. Res. A*, **579**, 15 (2007).
5. N.Y.Morgan, G.K.Marek, P.D.Smith et al., *Radiat. Res.*, **171**, 236 (2009).
6. Yanfei Lv, Xijun Wu, Daxiong Wu et al., *Powder Technol.*, **173**, 174 (2007).
7. G.Zimmerer, *Radiat. Meas.*, **42**, 859 (2007).
8. V.V.Vistovskyy, A.V.Zhyshkovych, N.E.Mitina, A.S.Zaichenko, A.V.Gektin, A.N.Vasil'ev, A.S.Voloshinovskii, *J. Appl. Phys.*, **112**, 024325 (2012).
9. Yu.M.Aleksandrov, V.N.Makhov, T.I.Syrejshchikova, M.N.Yakimenko, *Nucl. Instr. Meth. Phys. Res.*, **A261**, 158 (1987).
10. P.A.Rodnyi, A.Kh.Khandro, A.S.Voloshinovskii, G.B.Stryganyuk, *Opt. and Spectr.*, **103**, 568 (2007).
11. G.Blasse, B.C.Grabmaier, Luminescent Materials, Springer-Verlag, Berlin (1994).
12. E.Radzhabov, A.Nepomnyaschikh, *Solid State Commun.*, **146**, 376 (2008).
13. R.L.Amster, C.S.Wiggins, *J. Electrochem. Soc.*, **116**, 68 (1969).